

Supplemental information

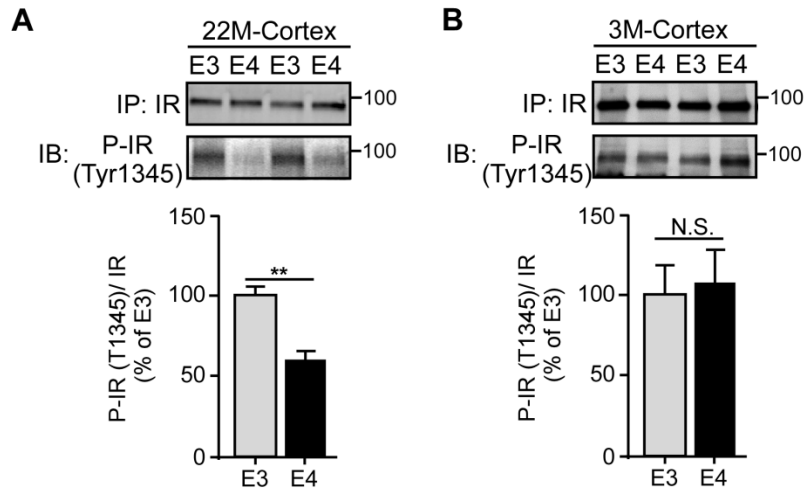


Figure S1: ApoE4 Impairs Cerebral Insulin Signaling in an Age-dependent Manner.

Related to Figure 1.

Brain lysates from the cortex of apoE3-TR and apoE4-TR mice (n=6-8 mice/genotype, mixed gender) at 22 months (A) and 3 months (B) of age were subjected to immunoprecipitation (IP) with an antibody specific to insulin receptor (IR). The amount of immunoprecipitated IR and p-IR (Tyr1345) was examined by Western blotting, and the ratio of p-IR/total IR was quantified. Data are expressed as mean \pm SEM relative to apoE3-TR mice. Two-tailed student's *t* test was used for statistical analysis. ** $p < 0.01$, N.S., not significant. Molecular mass markers in kilodaltons are shown.

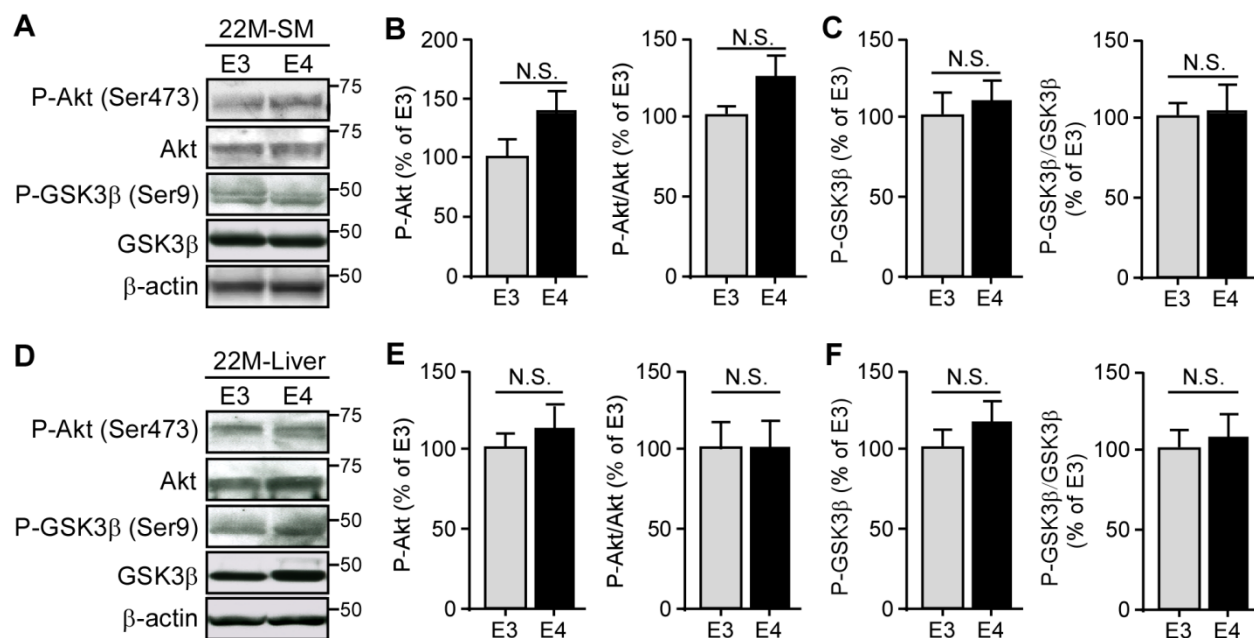


Figure S2: ApoE4 Does Not Affect Basal Peripheral Insulin Signaling in Aged Mice.

Related to Figure 1.

The amount of p-Akt (Ser473), total Akt, p-GSK3β (Ser9) and total GSK3β in the skeletal muscle (SM, A-C) and liver (D-F) of apoE3-TR and apoE4-TR mice (n=4-6 mice/genotype, mixed gender) at 22 months of age was examined by Western blotting. Results were normalized to β-actin. The ratios of p-Akt/total Akt and p-GSK3β/total GSK3β were quantified and calculated. Data are expressed as mean ± SEM relative to apoE3-TR mice. Two-tailed student's *t* test was used for statistical analysis. N.S., not significant. Molecular mass markers in kilodaltons are shown.

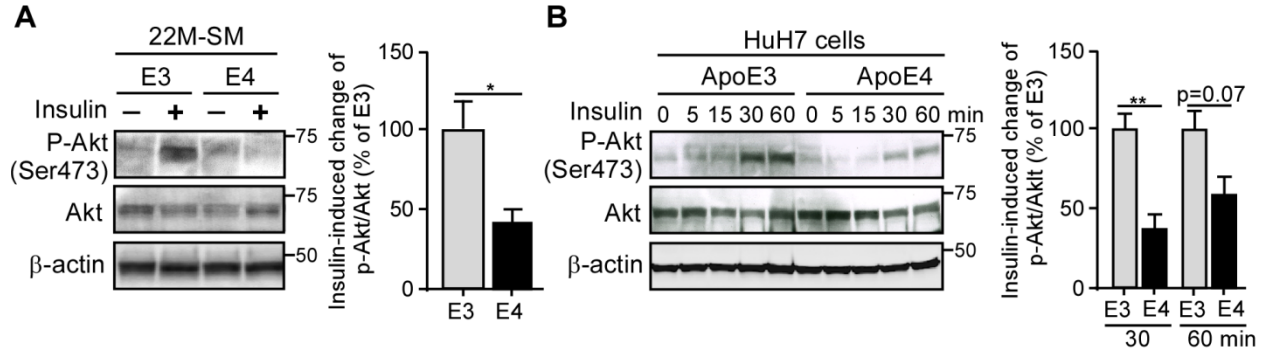


Figure S3: ApoE4 Reduces Peripheral Insulin Sensitivity. Related to Figure 3.

(A) The amount of p-Akt (Ser473), total Akt and β -actin in the skeletal muscle (SM) of old (22 months) apoE-TR mice was examined by Western blotting after insulin treatment through the inferior vena cava (n=5 mice/genotype, mixed gender). The change of p-Akt/total Akt ratio in response to insulin treatment was calculated. Data were normalized to apoE3-TR mice for comparison. (B) HuH7 cells were treated overnight with 50 nM recombinant apoE3 or apoE4 followed by insulin treatment (100 nM) for 0, 5, 15, 30 or 60 minutes. The amount of p-Akt (Ser473), total Akt and β -actin was detected by Western blotting (three independent experiments). The change of p-Akt/total Akt ratio after insulin treatment for 30 and 60 minutes was shown. Data were normalized to apoE3 treatment for comparison. Values are expressed as mean \pm SEM. Two-tailed student's *t* test was used for statistical analysis. **p* < 0.05; ***p* < 0.01. Molecular mass markers in kilodaltons are shown.

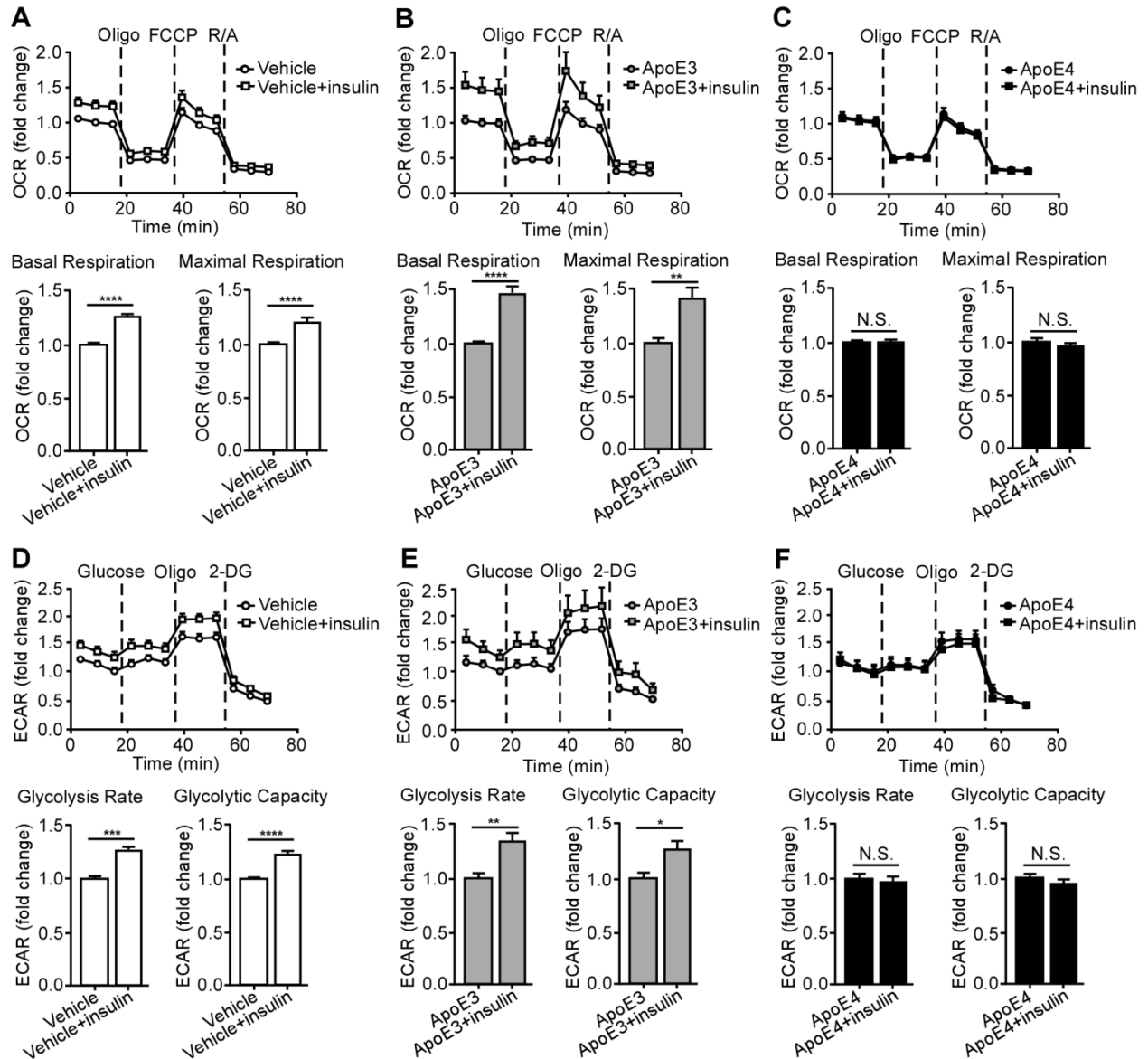


Figure S4: Lipidated ApoE4 Inhibits the Effect of Insulin on Mitochondrial Respiration and Glycolysis in Primary Neurons. Related to Figure 4.

Mitochondrial respiration (A-C) and glycolysis (D-F) were measured by Seahorse XFe96 analyzer in *ApoE*^{-/-} neurons treated overnight with vehicle (A, D) or 50 nM lipidated apoE3 (B, E) or apoE4 particles (C, F) followed by insulin (100 nM) treatment for 30 minutes.

(A-C) Oxygen consumption rate (OCR) was assessed over time after sequential injections of 2 μ M oligomycin, 1 μ M FCCP, and 5 μ M rotenone/antimycin A. Each value was derived from 10

to 12 repeats in two independent experiments and normalized to the third data point measurement of basal respiration (before oligomycin injection) for of non-insulin treatment group for comparisons. The basal respiration and the maximal respiration were calculated to compare the effect of insulin treatment.

(D-F) The extracellular acidification rate (ECAR) was assessed over time after sequential injections of glucose (10 mM), oligomycin (2 μ M) and 2-DG (50 mM). Each value was derived from 10 to 12 repeats in two independent experiments and normalized to the third data measurement of baseline glycolysis (before glucose injection) of non-insulin treatment group for comparison. The glycolysis rate and glycolytic capacity were calculated to compare the effect of insulin treatment. Data are expressed as mean \pm SEM. Two-tailed student's *t* test was used for statistical analysis. **** $p < 0.0001$; N.S., not significant. Oligo, Oligomycin; FCCP, Carbonyl cyanide-p-trifluoromethoxyphenylhydrazone; RA, rotenone/antimycin A.

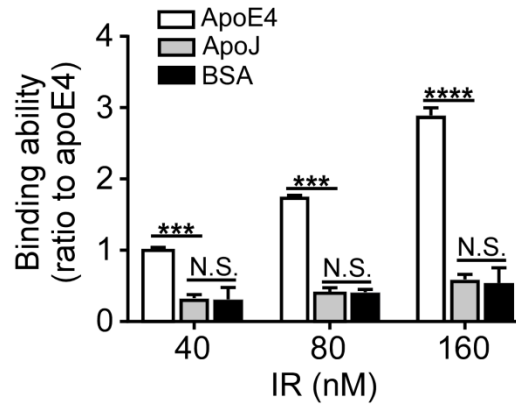


Figure S5: ApoJ Does not Bind to IR. Related to Figure 5.

The interaction between IR and apoJ was evaluated by solid-phase binding assay (three independent experiments). The binding of recombinant apoE4 and BSA to IR was included as positive and negative control, respectively. The values were normalized to the binding of apoE4 for comparison. Data are expressed as mean \pm SEM. One-way ANOVA with Tukey's multiple comparisons test were used in for statistical analysis. *** $p < 0.001$; **** $p < 0.0001$; N.S., not significant.

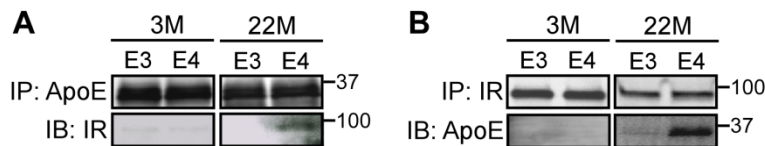


Figure S6: ApoE Interacts with IR in the Brain of Aged ApoE4 Mice. Related to Figure 5.

The interaction between apoE and IR *in vivo* was evaluated by co-immunoprecipitation. RIPA lysates from the cortex of apoE3 and apoE4-TR mice at 3 months and 22 months of age were immunoprecipitated (IP) with an apoE antibody (A) or an IR (B) antibody. The immunoprecipitates were then subjected to immunoblotting (IB) with IR or apoE antibody. Molecular mass markers in kilodaltons are shown.

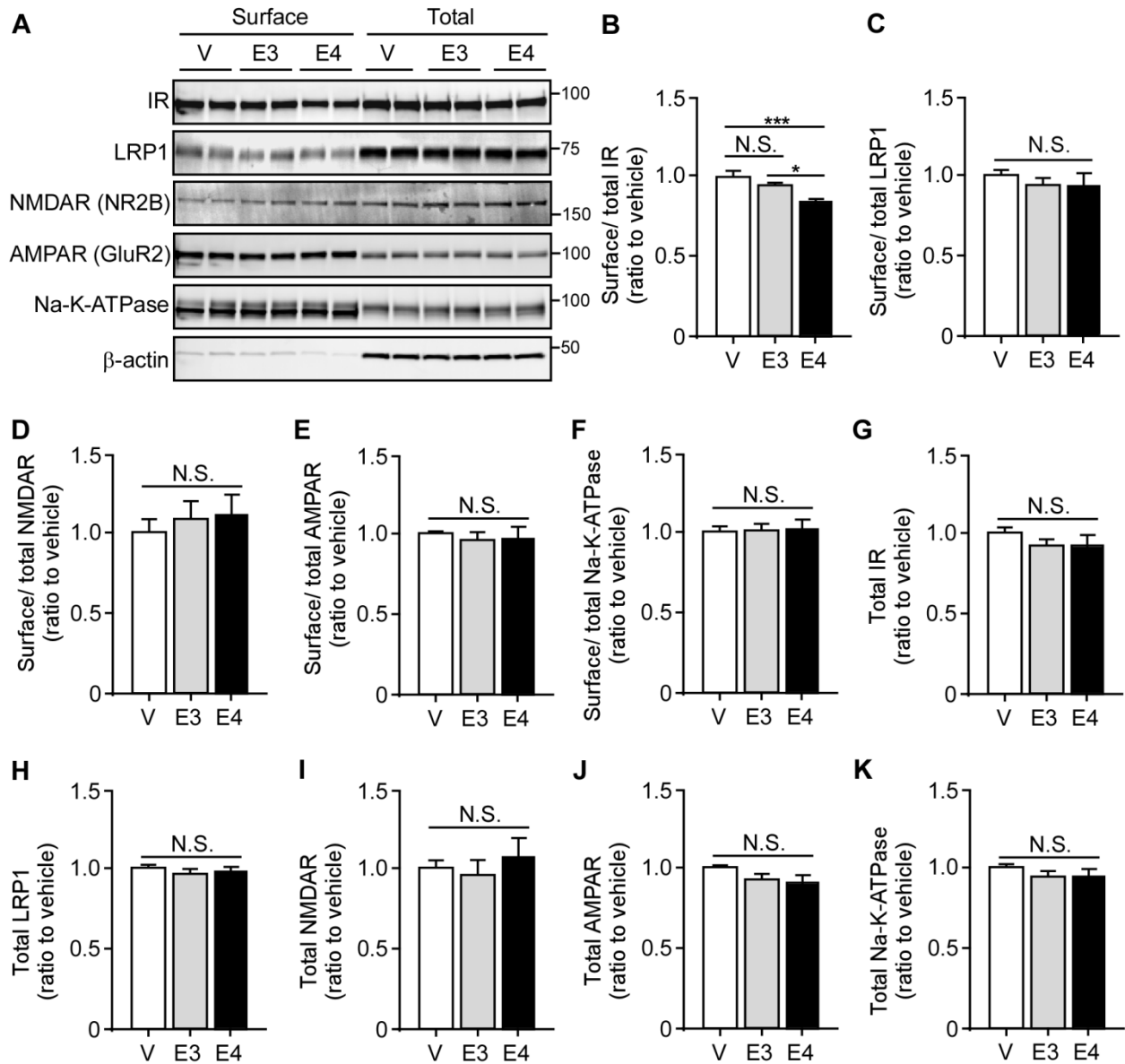


Figure S7: ApoE4 Suppresses the Amount of Cell Surface IR. Related to Figure 5.

(A) Primary *ApoE*^{-/-} neurons were treated overnight with recombinant apoE3 or apoE4 (100 nM), followed by cell surface biotinylation assay and Western blot analysis (three independent experiments). The cell surface IR, LRP1, NMDAR, AMPAR, Na-K-ATPase (A-F) and total IR, LRP1, NMDAR, AMPAR, Na-K-ATPase (A, G-K) were shown and the ratios of cell surface to total protein were calculated, respectively (B-F). The values were normalized to the vehicle-

treated group for comparison. All data represent mean \pm SEM. One-way ANOVA with Tukey's multiple comparisons test were used in for statistical analysis. * $p < 0.05$; N.S., not significant. Molecular mass markers in kilodaltons are shown.

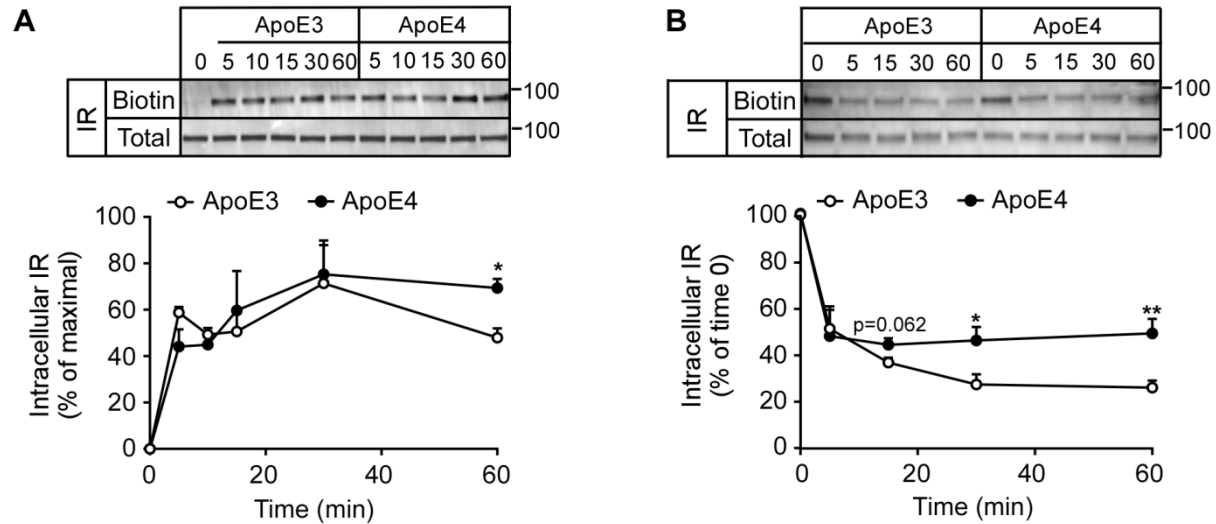


Figure S8: ApoE4 Impairs IR Trafficking. Related to Figures 5 and 6.

(A) Biotinylation assay was performed to examine the internalization of IR in primary *ApoE*^{-/-} neurons. Total IR and internalized IR (Biotinylated, labeled as Biotin) precipitated with streptavidin-conjugated beads were detected at various times (0, 5, 10, 15, 30, and 60 minutes) after apoE treatment (100 nM) (three independent experiments). The percentage of intracellular IR was calculated. All data represent mean \pm SEM. Two-tailed student's *t* test was used for statistical analysis. * $p < 0.05$. (B) Biotinylation assay was performed to examine the recycling of IR in primary *ApoE*^{-/-} neurons. After surface biotinylation, cells were treated with apoE for 30 minutes to allow the endocytosis to occur. ApoE was then removed and the recycling of IR was monitored at various times (5, 10, 15, 30, and 60 minutes) (three independent experiments). Cell-surface biotin was cleaved; thus, the decrease of intracellular (biotinylated) IR represents

receptor recycling. The percentage of the remaining intracellular IR at various times normalized to that at time zero was determined. All data represent mean \pm SEM. Two-tailed student's *t* test was used for statistical analysis. **p* < 0.05; ***p*<0.01. Molecular mass markers in kilodaltons are shown.

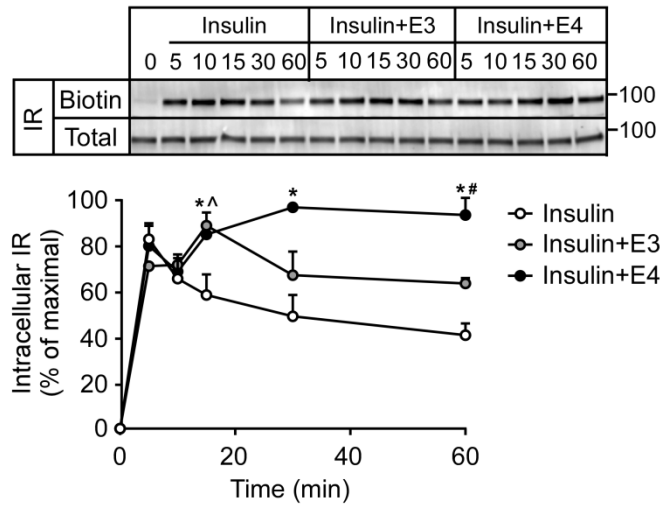


Figure S9: ApoE4 Interrupts Insulin-induced IR Trafficking. Related to Figures 5 and 6.

Biotinylation assay was performed to examine the internalization of IR in primary *ApoE*^{-/-} neurons. Total IR and internalized IR (Biotinylated, labeled as Biotin) upon insulin (100 nM) stimulation in the presence or absence of apoE isoforms (100 nM) were detected at various times (0, 5, 10, 15, 30, and 60 minutes) (three independent experiments). The percentage of intracellular IR versus total IR was calculated. All data represent mean \pm SEM. One-way ANOVA with Tukey's multiple comparisons test was used for statistical analysis. **p* < 0.05 (Insulin vs insulin+E4); ^*p*<0.05 (Insulin vs insulin+E3); #*p* < 0.05 (Insulin+E3 vs insulin+E4). All data represent mean \pm SEM. Molecular mass markers in kilodaltons are shown.

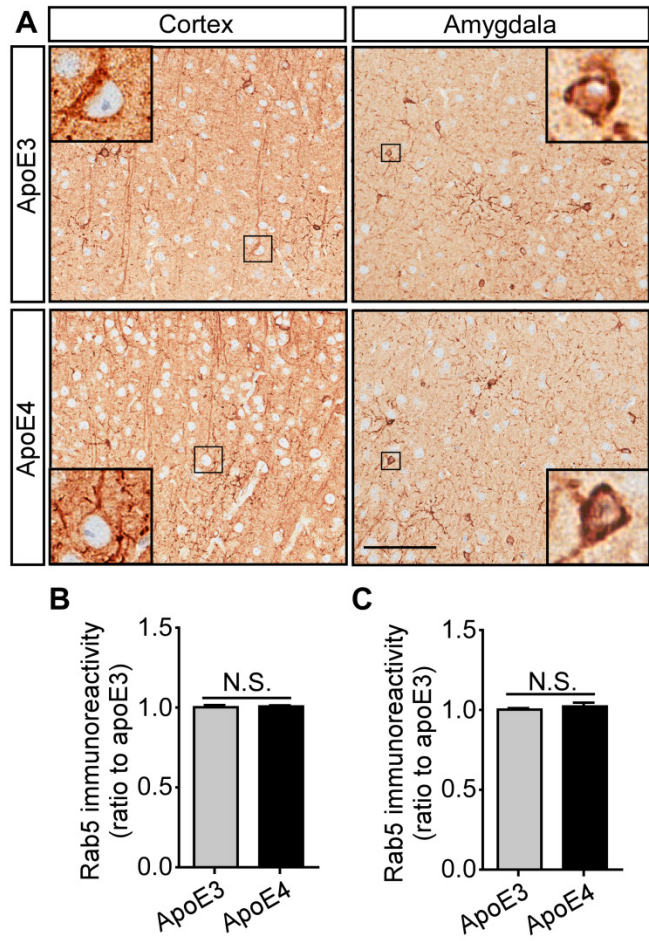


Figure S10: No ApoE Isoform Difference of Early Endosomal Marker in Young Mice.

Related to Figure 8.

Brain slices from apoE3-TR and apoE4-TR mice at 3 months of age were prepared, and the early endosome was examined by immunohistochemical staining for Rab5. The Rab5 expression pattern in the region of cortex and amygdala is shown (A). Scale bar, 100 μ m. (B, C) The immunoreactivity of Rab5 staining in the cortex and amygdala from apoE3- and apoE4-TR mice was quantified using Aperio ImageScope (n=6 mice/genotype, mixed gender). Data are expressed as mean \pm SEM relative to apoE3-TR mice. Two-tailed student's *t* test was used for statistical analysis. N.S., not significant.

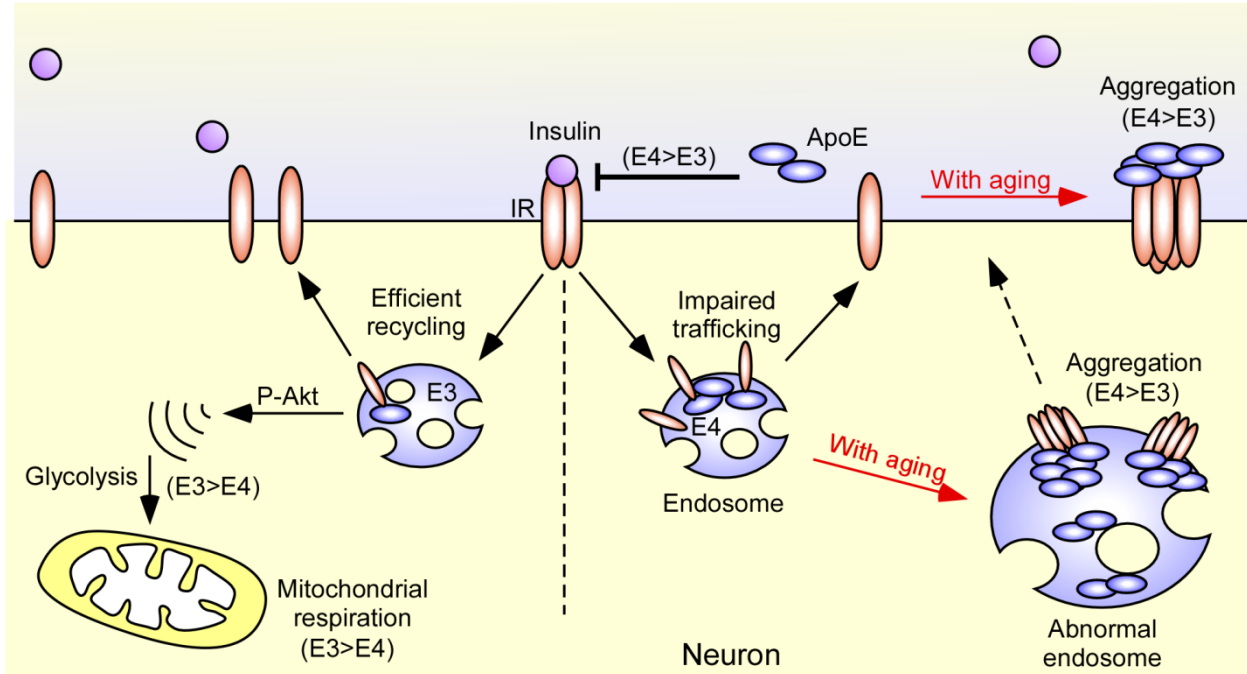


Figure S11: Proposed Mechanisms by which ApoE Isoforms Differentially Regulate Neuronal Insulin Signaling. Related to Figures 1-8.

ApoE4 suppresses neuronal insulin signaling activation by two potential mechanisms. First, apoE4 interacts with IR which blocks insulin-IR interaction. Second, defective trafficking of apoE4 sequesters IR in the endosomal compartments thereby less amount of IR is available on the cell surface for the action of insulin. ApoE3 is less aggregative thus allowing more IRs recycle back to cell surface. As a result, apoE isoforms differentially modulate insulin signaling and insulin-stimulated mitochondrial respiration and glycolysis in the neurons. With aging, the increased apoE4 aggregation and compromised endosomal function exacerbate the inhibitory effects of apoE4 on insulin signaling and related functions.